JMolMed

ORIGINAL ARTICLE

Curcumin nanoparticles inhibit corneal neovascularization

Nirparaj Pradhan[1] · Rajdeep Guha[2] · Sushovan Chowdhury[2] ·
Sudip Nandi[2] · Aditya Konar[2] · Sarbani Hazra[1]

Abstract

Corneal neovascularization is a leading cause for compromised vision. Therapeutic prevention of corneal neovascularization is a major clinical challenge, and there is a compelling need to seek effective and safe therapy for this pathology. This study is aimed to evaluate curcumin nanoparticle for prevention of corneal neovascularization. MePEG-PCL nanoparticles were successfully prepared and characterized. The nanoparticle of curcumin has shown increased efficiency in preventing angiogenic sprouting in vitro. Topical delivery of curcumin nanoparticle in the eye showed enhanced retention of curcumin in the cornea, and significant improvement in prevention of corneal neovascularization over free curcumin as graded clinically and by histopathology; suppression in the expression of VEGF, inflammatory cytokines, and MMP was evidenced in the treated cornea. Curcumin inhibited NFκB in LPS-induced corneal cells. Histopathology and scanning electron microscopy showed absence of any adverse change in the corneal structure following application of curcumin nanoparticle. Therefore, we conclude that curcumin nanoparticle can be a potential candidate for prevention of corneal neovascularization.

Key message

- Curcumin nanoparticles show enhanced retention of curcumin in the cornea.
- Curcumin NPs suppress the expression of VEGF, inflammatory cytokines, and MMP.
- Curcumin NPs prevent corneal neovascularization by suppressing the NFκB pathway.
- Curcumin NPs may be a promising candidate for prevention of corneal neovascularization.

Nirparaj Pradhan and Rajdeep Guha contributed equally to this work.

✉ Aditya Konar
adityakonar@yahoo.com

✉ Sarbani Hazra
shazrakon@yahoo.co.in

1   West Bengal University of Animal and Fishery Sciences, 37 & 68 Kshudiram Bose Sarani, Belgachia, Kolkata 700037, West Bengal, India

2   CSIR-Indian Institute of Chemical Biology, 4, Raja SC Mullick Road, Kolkata 700032, West Bengal, India

Background

Cornea, the major refractive surface of the eye is transparent and avascular for allowing light to pass into the retina. Lack of blood vessels and lymphatics also contributes significantly to the immune privilege of cornea and favors corneal transplantation. Avascular state of cornea is attributed by the strict balance of proangiogenic and antiangiogenic factors. Most important among these factors is vascular endothelial growth factor (VEGF), which is constitutively expressed in the corneal epithelium, endothelium, and limbal vascular endothelial cells, albeit at low levels, are normally buffered by soluble VEGFR-1 and VEGFR-3 to maintain avascularity and corneal clarity [1, 2]. Under pathological conditions such as infection, inflammation, and hypoxia, VEGF is expressed in infiltrating monocytes, neutrophils, and repair epithelium [3–7] that binds to VEGF receptor expressed in the limbal vascular endothelial cells and develop new blood vessels into the cornea leading to

corneal neovascularization. It is a major cause for compromised vision and a significant factor contributing to allograft rejection in corneal transplantation [8, 9]. The incidence of corneal neovascularization in the USA alone is estimated to be 1.4 million individuals [10]. It continues to remain a major clinical challenge.

Among the various therapeutic approaches identified so far, i.e., steroids, Cox 2 inhibitors, photodynamic therapy, fine needle diathermy, and anti-VEGF have proven to be effective in ameliorating corneal neovascularization [11]. Notwithstanding their clinical benefits, all are associated with major side effects. Steroids are associated with corneal thinning, ocular hypertension, and cataract that limit their use [12]; topical use of NSAIDs cause corneal ulceration and perforation [13]; photodynamic therapy and fine needle diathermy induce inflammatory response [14, 15]; and anti-VEGF therapy causes corneal thinning, reduced epithelial healing [16], and epithelial erosion [17]. Thus, there is a need to search for effective and safe therapy for corneal neovascularization.

Apart from its proangiogenic effect, VEGF also attract and recruit inflammatory cells, and inhibition of VEGF reduces inflammatory cells after corneal injury; on the other hand, reduced VEGF expression was evidenced following deletion of cytokine and chemokine receptors [3–5, 18–20]. Thus, a close cooperative linkage exists between VEGF expression and inflammation leading to corneal neovascularization. Nuclear factor κB (NFκB), a ubiquitous transcription factor which is cell- and tissue-specific, has been identified as a key factor in modulating ocular surface inflammation including corneal neovascularization [21]. Curcumin, the yellow extract from *Curcumina longa*, has demonstrated potential anti-inflammatory and antiangiogenic activity in various systems which has been shown to be mediated through inhibition of NFκB [22]; therefore, it promises to be a potential candidate for prevention of corneal neovascularization.

Bioavailability of drugs to the cornea remains a challenge as eye drops are continuously washed away by the tear fluid [23]; moreover, the unique anatomical feature of the cornea poses a strict physiological barrier to drug permeation [24]. Therefore, to be therapeutically effective, topical eye drops must be applied multiple times throughout the day which leads to the irritation of the eye and may also produce temporary blurred vision after application, causing discomfort [25]. We hypothesize that nanoparticle-mediated delivery can prolong the retention time of curcumin within the cornea and result in better therapeutic effect against corneal neovascularization.

This study aims to prepare and characterize curcumin nanoparticle and compare its antiangiogenic effect with free curcumin in vitro, to evaluate its retention in the cornea and its effect for prevention of corneal neovascularization in rat model vis a vis free curcumin and to identify the possible mechanism of antiangiogenic activity.

Methods

Preparation of nanoparticle Curcumin nanoparticles were prepared using solvent evaporation technique as described earlier for preparation of doxorubicin nanoparticle [26]. In brief, curcumin (Sigma, D1515) and poly(ethylene glycol) methyl ether-block-poly (e-caprolactone) (Sigma-Aldrich cat. no. 570338) (feed ratio 1:5) were simultaneously dissolved in ethyl acetate and added to a solution of 1 % didodecyldimethylammonium bromide (DMAB, Sigma, cat. no. 359025) drop by drop with constant stirring at 350 rpm on a magnetic stirrer until complete evaporation of ethyl acetate. Following 10-min sonication, the mixture was centrifuged in an ultracentrifuge (Thermo Scientific WX ULTRA 90) at 24, 000 rpm for 1 h. The NPs thus obtained were lyophilized (Virtis) and stored at 4 °C.

Characterization of nanoparticle Nanoparticles were characterized for drug loading, % yield, particle size, zeta potential, and surface morphology. Amount of curcumin in the supernatant was determined by HPLC and after subtracting it from the total curcumin used, the drug loading was calculated as [curcumin encapsulated / (curcumin used+polymer used)]×100, and % yield was calculated as weight of NPs obtained / (curcumin+polymer used). Particle size and zeta potential was determined by dynamic light scattering using Malvern ZetasizerNano (Malvern Instruments, Westborough, MA). Surface morphology of the nanoparticles was determined by atomic force microscopy. In brief, NPs were dispersed in water by sonication and a drop of it was placed on the freshly cleaved muscovite ruby mica sheet (ASTM V1 Grade Ruby Mica from MICAFAB, Chennai, India), air-dried, and imaged using a Pico plus 5500 ILM AFM (Agilent Technologies, USA) in amplitude and tapping mode.

Aortic ring assay Following euthanasia with excess of barbiturate, thoracic aorta from young mice were removed into a sterile petri dish containing ice-cold phosphate-buffered saline (PBS), surrounding tissues were removed and cut into 1-mm uniform slices. In a 48-well plate, 150 μl ECM gel was added and allowed to solidify at 37 °C for 30 min. A piece of aortic ring was placed on each ECM drop and another drop of ECM was placed on the ring and incubated at 37 °C for 30 min. In each well, 500 μl of human endothelial serum-free medium (GIBCO, Carlsbad, CA) supplemented with 2 % FCS, 50 units/ml penicillin, and 50 μg/ml streptomycin (Sigma) containing either only endothelial cell growth supplement (ECGS, final concentration 200 μg/ml, Sigma) or ECGS and different concentration of free curcumin and curcumin NP was added and incubated at 37 °C in a CO_2 incubator for 12 days. Rings were imaged on 4th, 8th, and 12th day under microscope (ECLIPSE TE 2000, Nikon, Japan), and the numbers of sprouts were counted.

Cell culture For culture of keratocytes, corneas were excised along with corneo-scleral junctions from young Sprague-Dawley rats; epithelial layers were removed with a sterile scalpel and cut into triangular-shaped wedges, using a single cut of the scalpel and placed on 35-mm tissue culture plate (Nunc); and cultured using Stemline™ keratinocyte medium (Sigma, S0196) containing human epidermal growth factor (0.1 ng/ml, Sigma), insulin (5 μg/ml, Sigma), hydrocortisone (0.5 μg/ml, Lonza), bovine pituitary extract (30 μg/ml, Sigma), and antibiotic mixture (50 IU/ml penicillin and 50 μg/ml streptomycin) (cat. no.15140, Gibco).

IkBα phosphorylation assay

Phosphorylation of IKBα was determined by a commercially available kit (R&D Systems; KCB4809) following manufacturer's protocol. Briefly, cells grown in 96-well plates were either left untreated or preincubated for 4 h with 10 μM free curcumin or nanoparticle containing 10 μM curcumin and treated with LPS (100 ng/ml) for 20 min. Following treatment, cells were fixed and permeabilized in the wells and simultaneously incubated with two primary antibodies: a phospho-specific antibody and a normalization antibody that is specific for GAPDH. Then, the cells were incubated with two secondary antibodies labeled with either horseradish-peroxidase (HRP) or alkaline phosphatase (AP). The fluorescence of the phosphorylated protein and GAPDH was measured using fluorescence plate reader with two different channels. Phosphorylated IKBα in each well were normalized to that of the total GAPDH in each well for the correction of well-to-well variations.

Nuclear localization of NFκB

Nuclear shuttling of NFκB was evaluated by immunocytochemistry. For this, corneal cells were cultured on glass cover slip for 24 h. Serum-starved cells were either left untreated or preincubated for 4 h either with 10 μM free curcumin or nanoparticle containing 10 μM curcumin and treated with lipopolysaccharide (LPS) (100 ng/ml) for 1 h. Cover slips were washed three times with Hanks' balanced salt solution (HBSS), and cells were fixed with 4 % paraformaldehyde for 20 min and rinsed with PBS. Then, the cells were permeabilized with 0.1 % Triton X-100 for 1 min on ice. Cells were overlaid with 3 % goat serum for 1 h at room temperature, rinsed with PBS with 0.03 % Triton-X (PBS-T), and incubated with anti-NFκB P65 antibody (1:100, Cell Signalling #E498) overnight at 4 °C in a humid chamber. Then, the cells were washed several times with PBS-T and incubated with secondary antibody (Alexa Fluor 568, Invitrogen, #A10042) for 2 h at room temperature. Cells were washed three times, counterstained with DAPI to visualize the nuclei, and

examined under fluorescence microscope (Leica DMI 4000B, Leica Microsystems, Germany).

Animal experiments The animal experiment was carried out with prior permission of Institutional Animal Ethics Committee and abiding by the tenets of Association of Research in Vision and Ophthalmology (ARVO). In the present study, experiment was conducted on clinically healthy Sprague-Dawley rats of either sex weighing about 200 g. All the rats were provided ad libitum feed and water, maintained under 12-h light and 12-h dark cycle. Routine clinical evaluation and preoperative ophthalmic examination of both eyes of all the animals was done prior to the experiment.

Animal model for neovascularization Rats were anesthetized with a combination of xylazine HCL (Xylaxine® Indian Immunologicals Ltd, Hyderabad, India) at 5 mg/kg and ketamine HCL (Ketamine 50®, Themis, Mumbai, India) at 50 mg/kg IM, one drop each of proparacain (Paracain 0.5 %, Sunways Pvt. Ltd, Mumbai, India), and tropacamide (Tropicacyl®, 1 %*w/v*, Sunways, Mumbai, India) was applied topically on the cornea. The corneal surface was touched for 10 s with cotton-tipped applicator soaked in silver nitrate solution and irrigated with PBS. Corneal defects were assessed by flourescein dye test. The rats were randomly divided into three groups and treated with either 20 μl of PBS (control), 20-μl solution containing 80 μg of free curcumin or 20-μl solution of curcumin NP containing equivalent amount of curcumin once daily for 14 consecutive days. A drop of ciprofloxacin eye drop (Ciplox®, Cipla Ltd, Mumbai, India) was instilled two times daily in all the affected eyes for 7 days. The eyes were examined everyday under stereo microscope (LeicaS8APO, Germany) and imaged on the 7th and 14th days. Animals were sacrificed by an overdose of barbiturate on different time points, and the corneas were collected; corneas excised on day 1, day 3, day 7, and day 14 and preserved in TRIzol® reagent for RNA isolation; and the corneas excised on day14 were preserved in −20 °C for Western blotting and HPLC, 10 % formalin for histopathology. In another set of animals, normal eyes were treated either with PBS or 20-μl solution containing 80 μg of free curcumin or 20-μl solution of curcumin NP containing equivalent amount of curcumin once daily for 14 consecutive days. The animals were sacrificed in similar way, and corneas were collected in 10 % formalin for histopathology and 2.5 % gluteraldehyde for scanning electron microscopy for evaluation of toxicity.

Quantitation of neovascularization Corneal neovascularization were quantified from the corneal images taken on the 14th day following standard procedure [27] with slight modification. The contrast level of images were set at which the neovascular area could be clearly delineated, areas with pixel densities similar to capillaries were selected and copied using

Adobe Photoshop. Using ImageJ, the images were converted to black and white applying binary mode; the total corneal area was then demarcated using the inner lining of the limbus as the external border. The neovascular (black pixels) and avascular (white pixels) areas were determined, and the fractional neovascular area were calculated (corneal neovascular area/total corneal area). Results are reported as mean fractional area ± SD. Statistical analysis was performed using one-way ANOVA.

Real-time PCR (qPCR) Total RNA was extracted from normal, control, free-curcumin-treated, and curcumin-NP-treated rat corneas using TRIzol® reagent (cat. no. 15596-018, Invitrogen, Life Technologies, USA) following manufacturer's protocol. Concentration of RNA was determined, and cDNA was transcribed according to manufacturer's instruction (Revert Aid™ First Strand cDNA Synthesis Kit, #K1622, Fermantas). Real-time PCR was performed with IL1β (F: GAGGACATGAGCACCTTCTTT, R: GCCTGT AGTGCAGTTGTCTAA), tumor necrosis factor alpha (TNF-α) (F: CTGAGTTCTGCAAAGGGAGAG, R: CCTC AGGGAAGAATCTGGAAAG, VEGF (F: TTGAGACCCT GGTGGACATC, R: CCAAAGCCAGCACATAGAGAG), metalloproteinase (MMP) 2 (F: GGTGGTGGTCACAGCT ATTT R: CCAGCCAGTCCGATTTGAT), MMP 9 (F: CCCAACCTTTACCAGCTACTC, R: GTCAGAACCGAC CCTACAAAG), and GAPDH (F: TCAACAGCAACTCC CACTCTTCCA, R: ACCCTGTTGCTGTAGCCGTATT CA) primers using SYBR® Premix Ex Taq™ (Perfect Real Time, TaKaRa #PR041A) in a real-time PCR cycler (ABI Prism 7500 Sequence Detection System; Applied Biosystems, Foster City, CA, USA). Relative messenger RNA (mRNA) levels in each sample were calculated after normalization to GAPDH mRNA expression using DD CT method as per manufacturer's methodology (Applied Biosystems, Foster City, CA, USA).

Western blotting Corneas were washed with ice-cold PBS and homogenized in an homogenizer with ice-cold lysis buffer (50 mM Tris–HCl, pH 7.2, 150 mM NaCl, 2 mM EDTA, 10 % (v/v) NP-40, 1 mM sodium orthovanadate, 50 mM sodium pyrophosphate, 100 mM sodium fluoride, 0.01 % (v/v) aprotinin, 4 μg/ml of pepstatin A, 10 μg/ml of leupeptin, 1 mM phenylmethylsulfonyl fluoride, PMSF) for 5 min and centrifuged at 15,000×g for 10 min. Supernatant was obtained and concentration of protein was determined by Bradford method. Laemmli sample buffer was added to the lysate supernatant and boiled for 5 min. Equal quantity of proteins from each sample were separated by SDS-PAGE (10 %) gel and transferred to polyvinylidene fluoride membranes (PVDF; Millipore, Billerica, MA). Membranes were blocked in blocking buffer (5 % skimmed milk powder in TBST (0.1 M Tris, pH 9.5, containing 0.05 M MgCl$_2$ and 0.1 M

NaCl and 0.1 % Tween 20) for 2 h, incubated overnight at 4 °C with primary antibodies against VEGF-A (1:200, Novus Biologicals, NB600-1003) or beta actin (1:500, Cell Signalling, #4970), washed three times with TBST, and further incubated with HRP-conjugated secondary antibody (1:5000, Immunopure antibody, Thermo Scientific, #31460). Membranes were washed in TBST, and specific antigen-antibody complexes were developed by using SuperSignal® West Dura extended duration substrate, Thermo Scientific, #34076), and the chemoilluminescence was detected by a ChemiDoc system (Gel Logic 4000 PRO, Carestream Health, Canada).

Histopathology Corneas were fixed in formalin, cleared in xylene, dehydrated in graded alcohol, and embedded in paraffin. Five-micron-thick sections were prepared, stained with hematoxylin and eosin, and examined under microscope (Leica DM 2500). Corneal sections from eyes induced for angiogenesis and treated with either PBS or free curcumin and curcumin NP were examined for presence of blood vessels; number of vessels observed in ten microscopic fields from each group is presented as mean ± SD. Corneal sections from normal eyes treated either with PBS or free curcumin or curcumin NP were evaluated for toxicity.

Scanning electron microscopy The corneas from normal eyes treated either with PBS or free curcumin or curcumin NP were preserved in 2.5 % gluteraldehyde. Corneas were treated with graded alcohol and imaged under scanning electron microscope TESCAN Vega II LSU (TESCAN Digital Microscopy Imaging) after gold sputtering.

HPLC for quantification of curcumin in the cornea

The corneas were collected on 14th day 6 h after the last treatment and stored at −20 °C until further use. HPLC was done following a method used for determination of doxorubicin in plasma and tissues [28]. In brief, corneal samples were homogenized in 1 ml of 20 mM K$_2$HPO$_4$ (pH 3.8) and 250 μl of acetone was added to each homogenate to precipitate the protein in the samples. The homogenates were centrifuged at 2000 rpm, and the supernatants were collected in fresh microcentrifuge tubes. The samples were lyophilized, and the residue was dissolved in 200 μl of the mobile phase and introduced into the HPLC system for analysis.

The mobile phase consisted of 50 mM potassium dihydrogen phosphate (pH 3.5): acetonitrile as 40:60 v/v and was pumped isocratically at a flow rate of 1 ml/min.

The amount of curcumin in the samples was calculated from a standard curve obtained by using different known concentrations of curcumin. The curve was linear and the equation relating the areas of the peaks to the concentration of curcumin was obtained as $Y=28.51X$, $R^2>0.823$, where $Y =$

Table 1 Physicochemical characteristics of the nanoparticles

Feed ratio	Average particle size (nm)	Zeta potential (mV)	Polydispersity index	% Encapsulation	% Yield	Drug loading %
20:100	90.92±0.77	−20.1±2.31	0.260±0.05	91.9±0.09	97.84±0.84	15.39±0.74

Data presented as mean±SD

area of the peaks and X = concentration of curcumin in the samples.

Statistical analysis All values, unless otherwise stated, are expressed as mean±SD. The minimum number of replicates for all measurements was at least 3. Comparison between groups were done by one-way analysis of variance, and the significance level was set at $p<0.05$.

Results

Characterization of curcumin loaded MePEG-PCL nanoparticle Considerably high encapsulation efficiency and % yield was obtained. The nanoparticles were characterized for particle size, zeta potential, and polydispersity index using dynamic light scattering. The particle size, zeta potential, and PDI are presented in Table 1. Atomic force
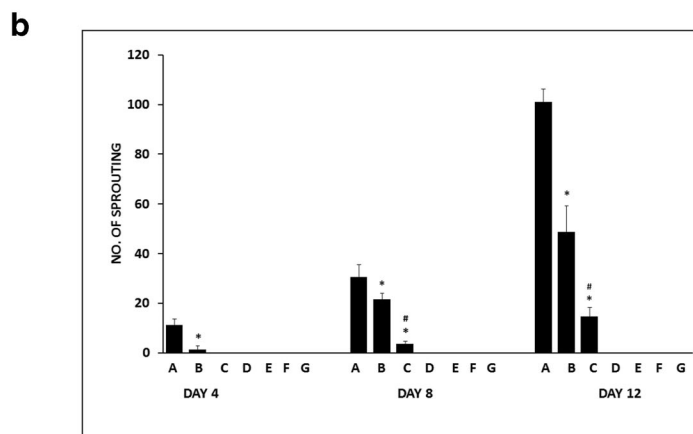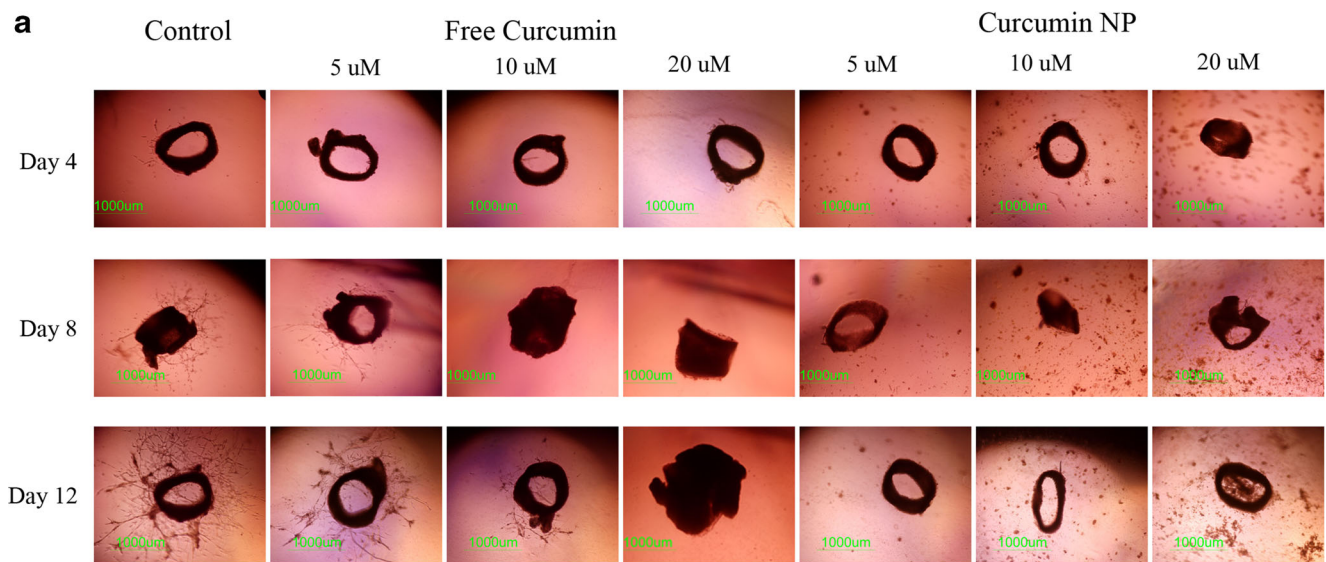

Fig. 1 Curcumin NP shows increased efficiency in preventing angiogenesis compared to free curcumin. **a** Culture of aortic ring in presence of ECGS resulted in appearance of angiogenic sprouts on the fourth day that significantly increased on day 8, and on day 12, they had grown into tube-like structures. Curcumin dose- and time-dependently inhibited angiogenic sprouting. Curcumin NP completely inhibited the sprouting at the lowest dose and exhibited better effect than free curcumin. **b** Graphical representation of number of sprouts: *A*, control; *B* 5 μM; *C*, 10 μM; *D*, 20 μM free curcumin, *EFG* curcumin NP containing 5, 10, and 20 μM curcumin, respectively. Data represented as mean±SD; *$p<0.05$ vs control, #$p<0.05$ vs 5 μM free curcumin; $N=6$
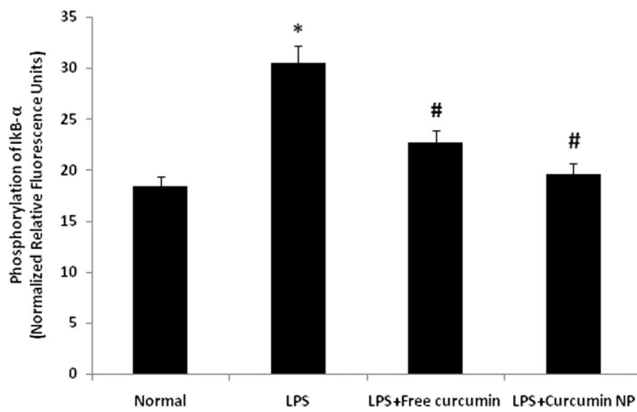
Fig. 2 Curcumin prevents LPS induced phosphorylation of IKBα in keratocytes. Corneal keratocytes were treated with LPS that resulted in increased phosphorylation of IKBα, pretreatment with curcumin and curcumin NP prevented this increased phosphorylation. Data presented as mean±SD, *$p < 0.05$ vs normal, #$p < 0.05$ vs control (LPS)

microscopy (AFM) showed that the particles were spherical and had smooth surface (Suppl. Fig. 1).

Curcumin NPs prevent angiogenic sprouting Culture of aortic ring in the presence of ECGS resulted in appearance of angiogenic sprouts on the fourth day that significantly increased on day 8, and on day 12, they had grown into tube-like structures. Aortic rings cultured in presence of ECGS and 5 μM free curcumin also generated sprouts on day 4 that increased on day 8 and day 12 but remained significantly

lower compared to the only ECGS treated rings. In ECGS and 10 μM free-curcumin-treated rings, first appearance of sprout was observed on day 8 that increased on day 12; however, the number was significantly lower than the only ECGS-treated rings. No sprouting was observed from the rings treated with ECGS and 20 μM free curcumin. Therefore, curcumin prevented angiogenic sprouting in the cultured aortic ring in dose- and time-dependent manner, whereas none of the cultured rings treated with ECGS and curcumin NP generated any sprout even on 12th day (Fig. 1). This indicated improved efficiency of curcumin NP than free curcumin in preventing angiogenesis.

Curcumin NPs suppressed phosphorylation of IKBα In resting stage, NFκB is retained within the cytoplasm by inhibitory subunit IKBα; after activation, IKBα is phosphorylated and subsequently degraded, as a result NFκB becomes free and translocate to nucleus. Therefore, we examined whether LPS increases the phosphorylation of IKBα and if curcumin or curcumin NP can prevent the phosphorylation. Our data clearly showed that treatment of corneal cells with LPS increased phosphorylation of IKBα whereas curcumin NP as well as the free curcumin prevented the phosphorylation of IKBα (Fig. 2).

Curcumin NPs prevented LPS induced activation and nuclear translocation of NFκB Nuclear localization of NFκB
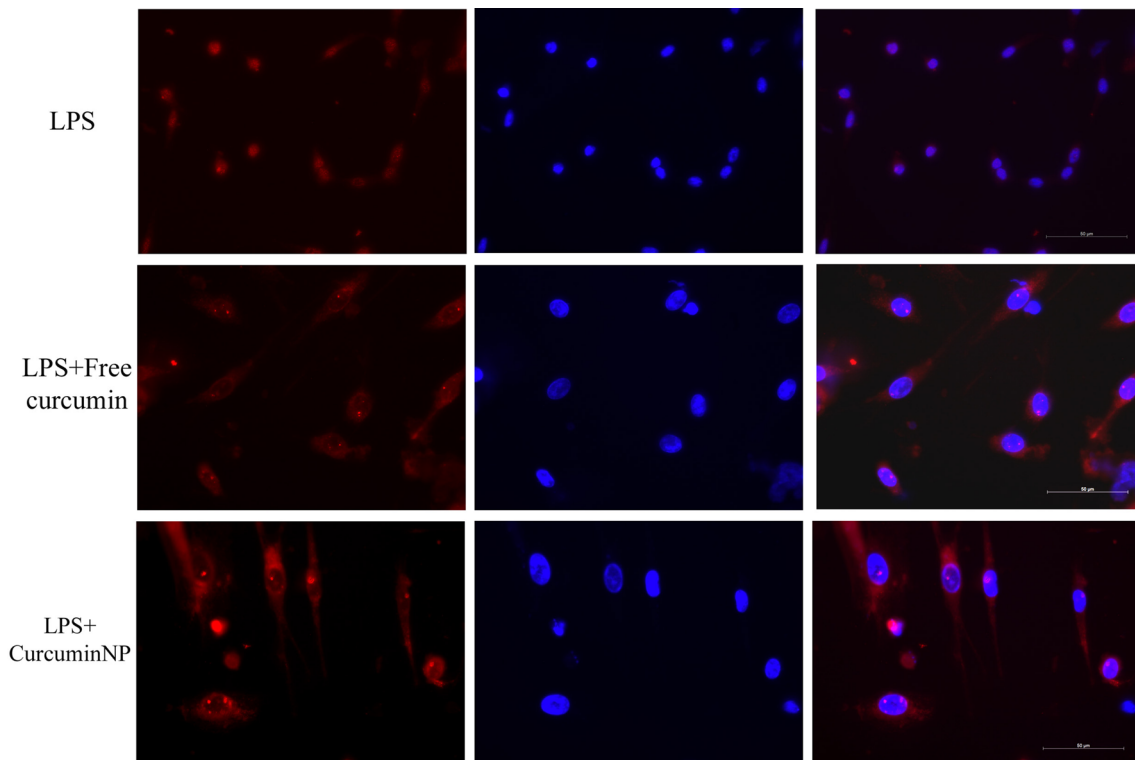

Fig. 3 Curcumin prevents nuclear localization of NFκB. Treatment of keratocytes with LPS shows localization of NFκB within the nucleus, whereas pretreatment with curcumin and curcumin NP retains it within the cytoplasm

in corneal cells was examined by immunocytochemistry with NFκB P65. In LPS-treated cells, NFκB was detected in the nucleus whereas in corneal cells pretreated with curcumin and curcumin NP, NFκB was observed to be localized in the cytoplasm (Fig. 3). Therefore, curcumin NP blocked nuclear translocation of NFκB.

Curcumin NPs prevent corneal angiogenesis

Clinical evaluation Clinical examination showed extensive neovascularization on the control and free-curcumin-treated corneas, although the extent appeared to be lesser on the latter as compared to the control. However, curcumin-NP-treated eyes showed a distinct reduction in neovascularization. The images taken on 14th day after induction were analyzed with ImageJ software. The analysis showed huge neovascular area on the control and free-curcumin-treated corneas and a

significant ($p<0.05$) reduction in the neovascular area on curcumin-NP-treated corneas. The analysis supported the clinical observation (Fig. 4a, b).

Histopathology Histology showed huge number of capillaries in the corneal sections from control as well as free curcumin treated eyes. However, the corneal sections from curcumin NP treated eyes showed only very few capillaries and the reduction was significant ($p<0.05$) compared to control as well as free curcumin treated corneas, that clearly indicated increased efficacy of curcumin NPs for prevention of corneal neovascularization (Fig. 4c, d).

Curcumin NPs suppressed increased expression of inflammatory cytokines Modulation of inflammatory cytokines was evaluated on first, third, and seventh days. Real-time PCR showed significantly ($p<0.05$) increased expression of IL1β and TNF-α on the third as well as seventh days in
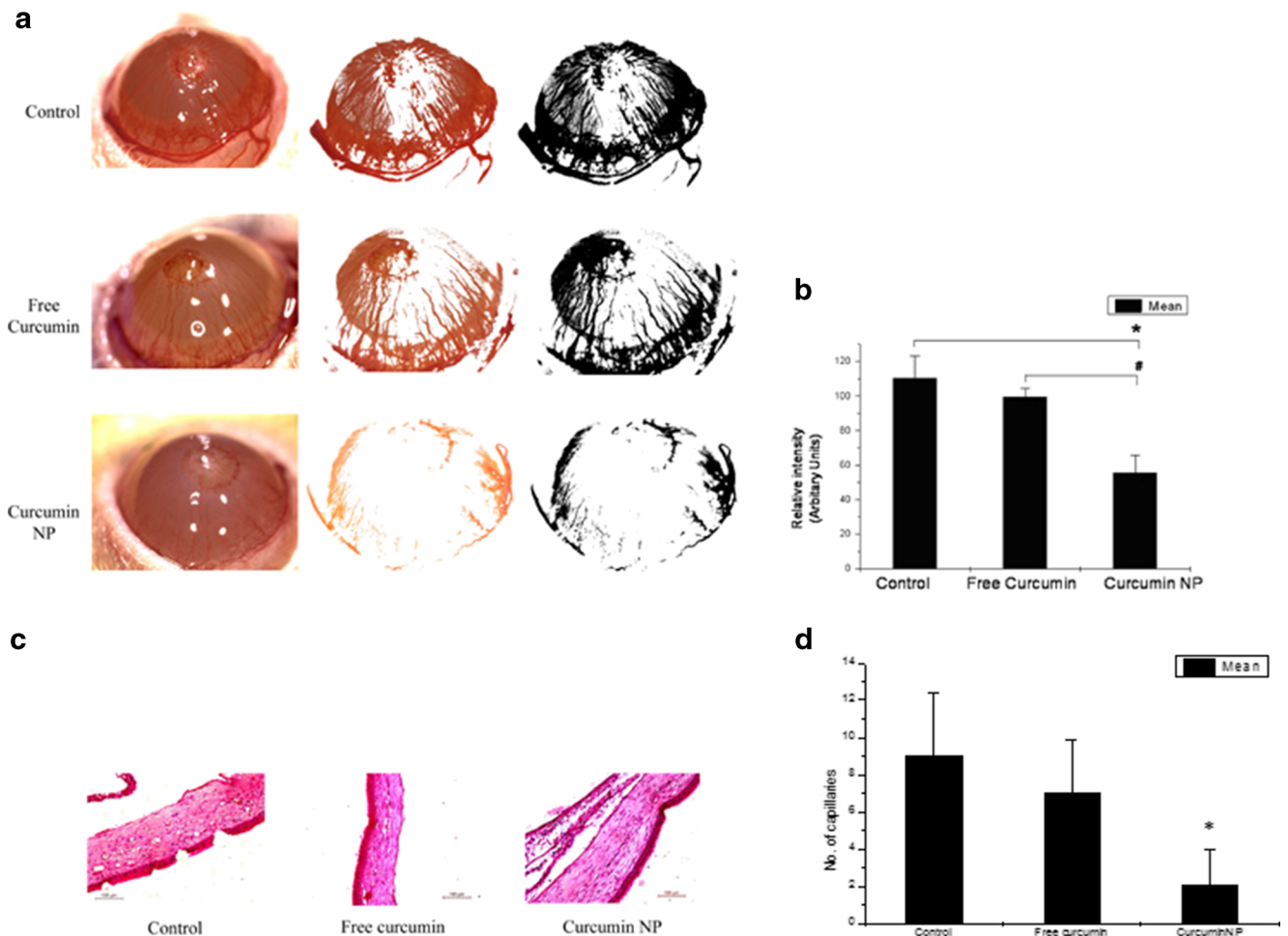

Fig. 4 Curcumin NP prevents corneal neovascularization. **a** Corneal images show huge angiogenesis in control cornea and reduction in free curcumin and curcumin NP treated corneas. Binary images are also presented. **b** Areas of neovascularization were determined by ImageJ software and represented graphically. Data are presented as mean fractional area±SD. *$p<0.05$ vs control, #$p<0.05$ vs free curcumin; $N=6$. **c** Histopathology of control cornea also shows huge increase in the number of capillaries and lesser number in free curcumin treated corneas, whereas curcumin NP treated cornea shows only very few capillaries. **d** Bar diagram representing number of capillaries. Data are presented as mean±SD.*$p<0.05$ vs control

control corneas compared to normal corneas. A significant ($p<0.05$) and progressive reduction in the expression of both IL1β (Fig. 5a) and TNF-α (Fig. 5b) were observed following curcumin NPs treatment.

Curcumin NPs prevent increased expression of VEGF Expression of VEGF was assessed in the corneas after 14 days. A significant ($p<0.05$) increase in the expression of VEGF mRNA in the corneas from control rats was observed compared to normal rats by real time PCR. The VEGF mRNA expression was reduced ($p<0.05$) in free curcumin treated corneas compared to the control animals.

A further significant ($p<0.05$) reduction of mRNA expression was detected in curcumin NPs treated corneas compared to both control as well as free curcumin treated animals (Fig. 6a). The Western blot analysis also showed increased VEGF protein expression in control corneas and its significant ($p<0.05$) reduction in curcumin NP treated corneas (Fig. 6b).

Curcumin NPs suppress increased expression of MMPs Real-time PCR analysis showed significant ($p<0.05$) increase in the expression of MMP2 and MMP9 in control corneas compared to normal corneas.
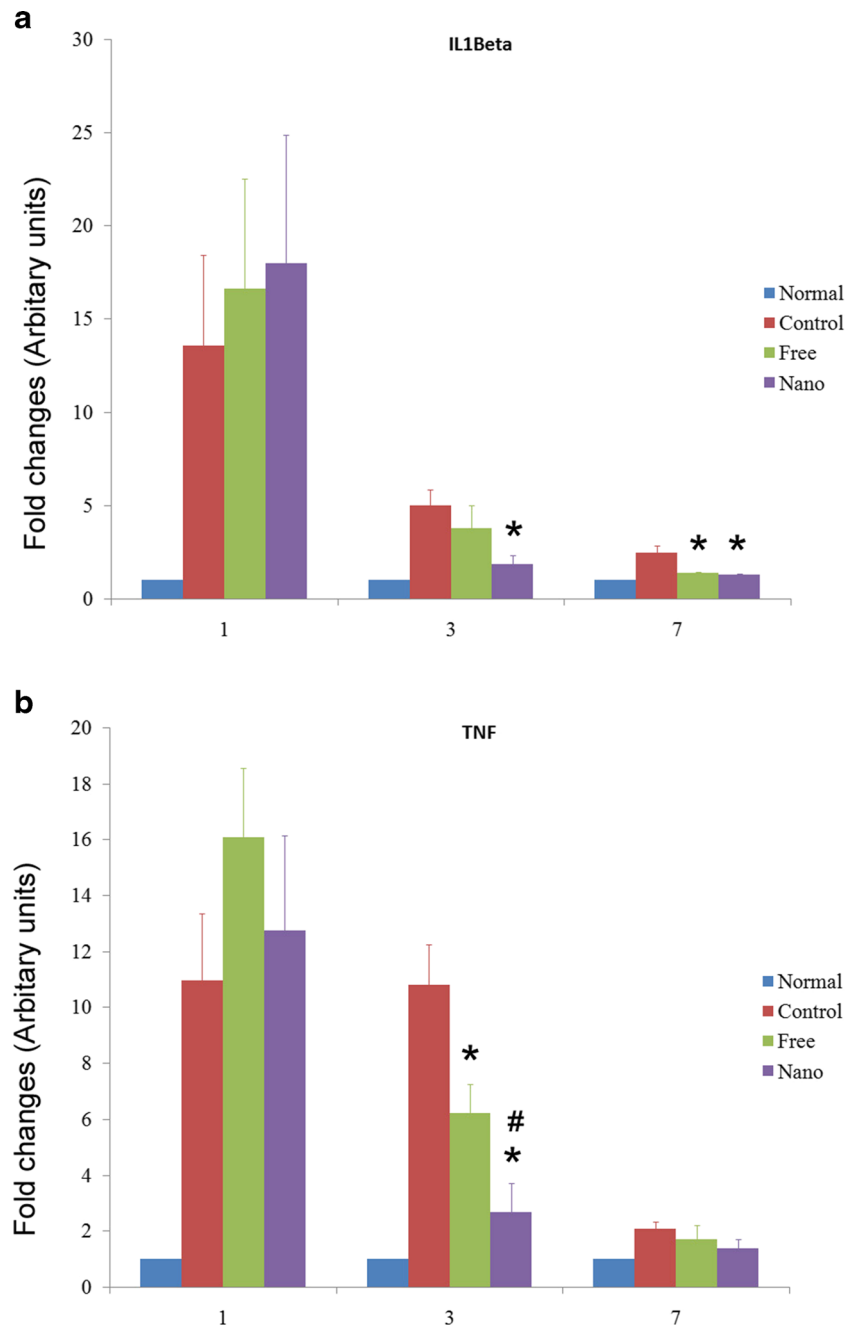
Fig. 5 Curcumin prevents increased inflammation in the cornea. Real-time PCR shows huge increase in the expression of IL1β and TNF-α in control, free curcumin, and curcumin NP treated corneas on day 1, treatment of curcumin NP significantly decreased the expression of IL1β (**a**) and TNF-α (**b**) on day 3 and day 7 compared to control and free curcumin treated corneas. Data is expressed as mean±SD; *N*=3; *$p<0.05$ vs control, #$p<0.05$ vs free curcumin

Fig. 6 Curcumin NP prevents increased expression of VEGF in the cornea. Real-time PCR (**a**) as well as Western blot analysis (**b**) show increased expression of VEGF in the control cornea which is prevented in free curcumin and curcumin NP treated corneas. Data is expressed as mean±SD; $N=3$; *$p<0.05$ vs normal, #$p<0.05$ vs control, @$p<0.05$ vs free curcumin
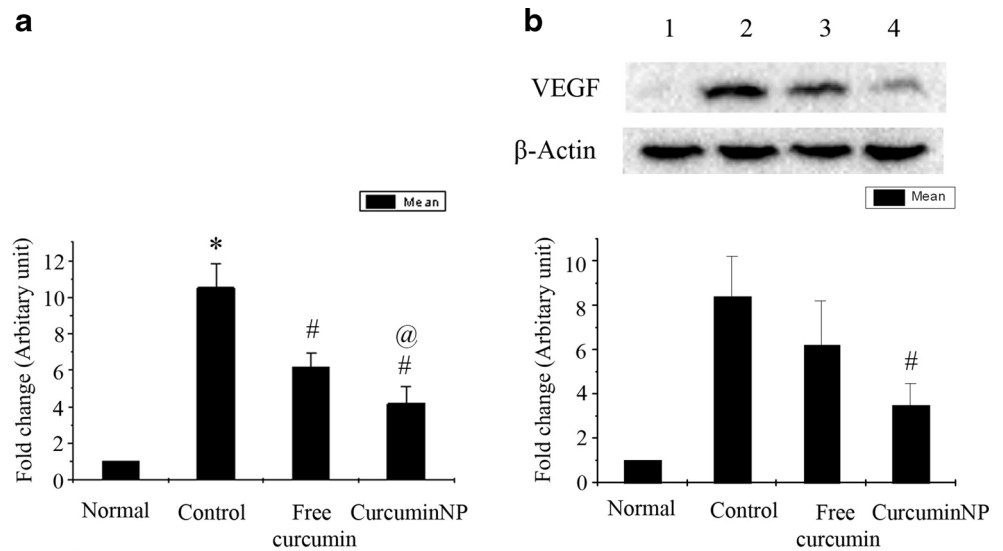
A significant ($p<0.05$) prevention of MMP2 (Fig. 7a) as well as MMP9 (Fig. 7b) expression was observed in free curcumin and curcumin NP treated corneas compared to control, the expressions in curcumin NP treated corneas were significantly ($p<0.05$) lower compared to free curcumin treated corneas.

Curcumin NP does not affect the histology and ultrastructure of the normal cornea Corneas from normal eyes were treated with either PBS or free curcumin or curcumin nanoparticle to evaluate their effect on normal corneas. Histology sections from free curcumin and curcumin NP treated cornea showed normal architecture of cornea, similar to that of PBS treated cornea (Fig. 8a).

Scanning electron microscopy showed normal architecture of epithelial and endothelial cells in the cornea from free curcumin and curcumin NP treated eyes that resembled the PBS treated normal cornea. The cellular junctions were also

found to be unaltered in both the treatment groups (Fig. 8b). Therefore, treatment of corneas with either free curcumin or curcumin NP did not change its ultrastructure.

Nanoparticle-mediated delivery increased availability of curcumin in the cornea On 14th day, 6 h after last treatment, presence of curcumin within the cornea was quantified by HPLC. Higher amount of curcumin was detected in the corneas treated with curcumin NP compared to the corneas treated with free curcumin (19.88+4.9 vs 0.65+0.65 μg). Therefore, nanoparticle-mediated delivery of curcumin prolonged the availability of curcumin within the cornea.

Discussion

The attributes of nanoparticle-mediated drug delivery promises remarkable contribution in ophthalmology and for
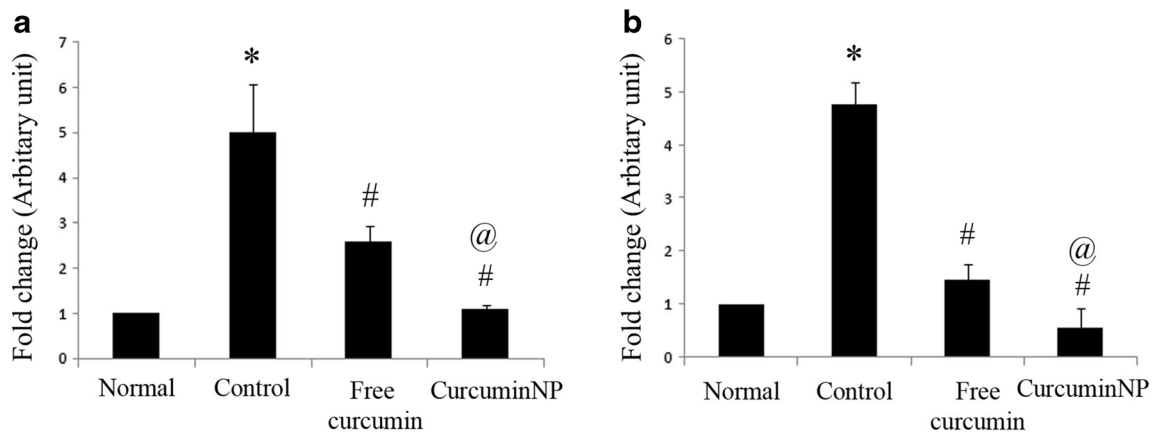

Fig. 7 Curcumin NP prevents increased expression of MMPs in the cornea. Real-time PCR shows increased expression of MMP2 (**a**) and MMP9 (**b**) in the control cornea which was prevented in free curcumin and curcumin NP treated corneas; the expressions in curcumin NP treated corneas were significantly lower than free curcumin treated corneas. Data is expressed as mean±SD; $N=3$; *$p<0.05$ vs normal, #$p<0.05$ vs control, @$p<0.05$ vs free curcumin
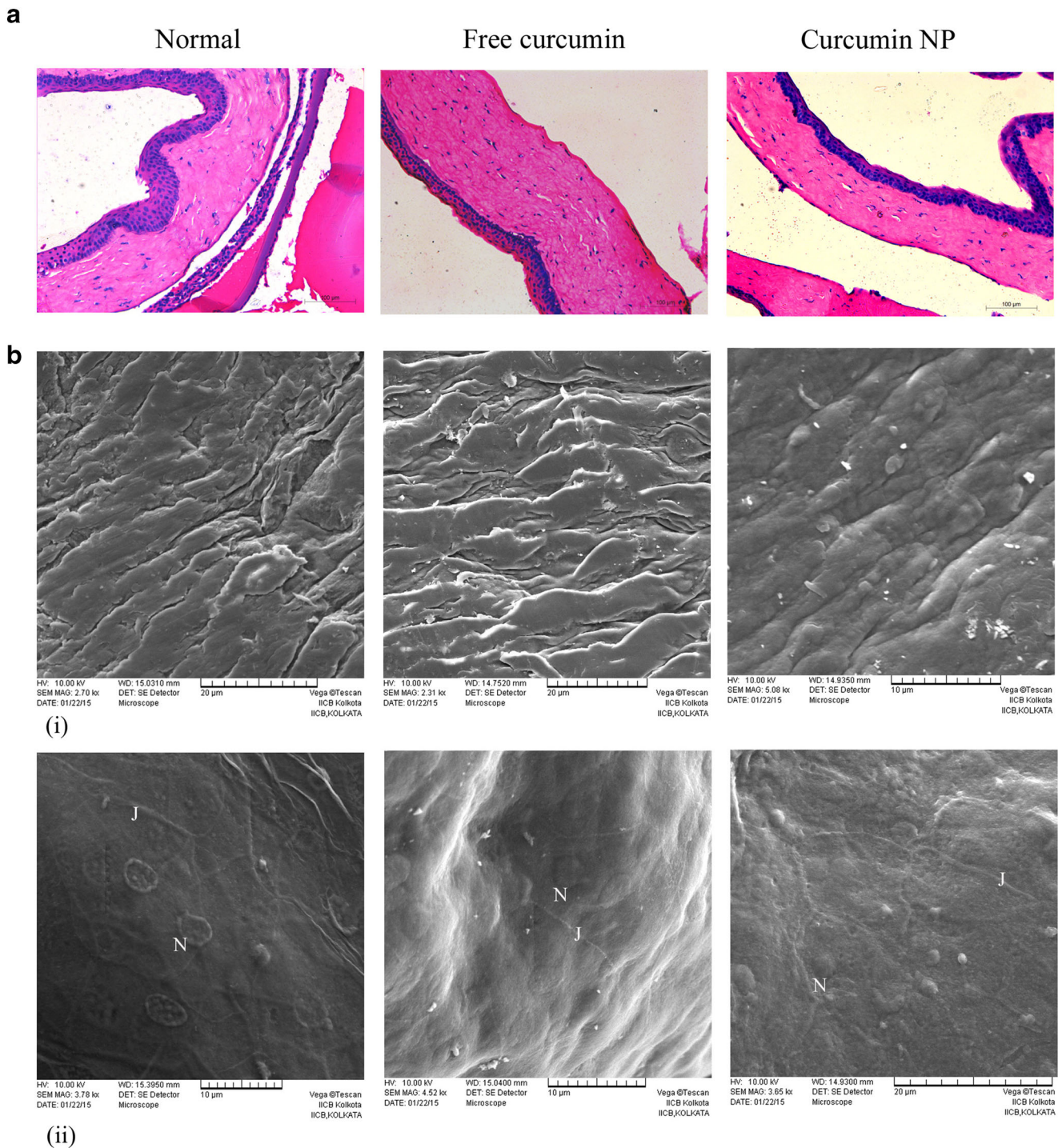
a

b

Fig. 8 Curcumin NPs and free curcumin does not change the normal architecture of cornea. **a** Histology sections of corneas from eyes treated with free curcumin and curcumin NP shows normal corneal architecture as corneas from PBS-treated eyes. **b** Scanning electron microscopy also shows that the epithelial (*i*) and endothelial (*ii*) cells of the corneas retained normal architecture following either free curcumin or curcumin NP treatment; cell nucleus (*N*) and tight junction (*J*) of the endothelial can be seen clearly. The architecture is comparable with normal cornea

prevention of corneal neovascularization in particular [11]. In this study, we have shown the advantage of curcumin NP over free curcumin for preventing corneal neovascularization in a rat model of chemical injury.

The MePEG-PCL curcumin NPs were smooth and without cracks; the zeta potential and polydispersity index were appropriate for conferring its stability and prevention of aggregation. Our in vitro study with free curcumin has shown

significant dose-dependent as well as time-dependent reduction of angiogenic sprouting in aortic ring assay. We observed complete inhibition of sprouting with 20 μM free curcumin, whereas same effect was evidenced with 5 μM curcumin NP. Bian et al. [29] reported prevention of human umbilical vein endothelial cell (HUVEC) proliferation by free curcumin. Aortic ring assay mimics in vivo angiogenesis more closely as it simulates the proteolytic activity, cell migration along with proliferation of endothelial cells. Irrespective of the assay system, curcumin inhibited endothelial cell proliferation and prevented angiogenesis and curcumin NP showed increased efficiency in our study.

Chemical injury is a prevalent cause of corneal neovascularization clinically [30, 31]. In experimental setup, various models are used for producing corneal angiogenesis, some commonly used are, the suture induced, and chemical injury. Among these, chemical injury model for corneal neovascularization has been widely used due to the ease with which it can be induced and easy visualization [32]. In this study, corneal angiogenesis was induced with silver nitrate to obtain a robust model for mimicking clinical inflammatory corneal neovascularization. Considering topical eye drops as the most accessible and least invasive delivery route to the eye, we choose to deliver curcumin NP topically.

We observed significant reduction in corneal neovascularization following once daily treatment with curcumin NP for 14 days. Reduction of neovascularization with once daily free curcumin was not remarkable; Kim et al. [33] reported prevention of CNV following multiple daily dosing with curcumin in rabbit eye. Histopathology of corneal sections also supported the clinical findings; corneal sections from curcumin NP treated corneas showed only very few capillaries as opposed to huge number of capillaries in control and free curcumin treated corneas. Consistent with these findings, we also registered increased expression of VEGF in the control cornea and its hierarchical reduction with free curcuin and curcumin NP. Curcumin NPs also demonstrated significant reduction of corneal inflammation. Both suppression of inflammation and VEGF played important role in prevention of corneal neovascularization [34]; however, their individual contribution could not be uncoupled in this study. Matrix metalloproteinase is another important player in inducing corneal neovascularization [35]; therefore, we sought to evaluate its expression following treatment with curcumin NPs and observed significant reduction.

Our study also demonstrates that curcumin and curcumin nanoparticles inhibit nuclear localization of NFκB and thereby exhibit anti-inflammatory and antiangiogenic activity in corneal cells.

Though curcumin has exhibited potential antiangiogenic activity in various systems including the eye [33, 36–38], major concern with curcumin for topical use on the cornea is its poor bioavailability [39], attributed by its chemical nature,

and like most ophthalmic drops, its reduced retention time on the cornea.

Interestingly, consistent with our hypothesis, curcumin NP have demonstrated significant improvement in activity over free curcumin; this is further supported by our HPLC data which shows increased availability of curcumin in curcumin NP treated corneas compared to those treated with free curcumin. This is the first study that demonstrates advantage of using curcumin NP over free curcumin for prevention of corneal neovascularization via topical route.

Histopathology sections and scanning electron microscopy of corneas showed treatment either with free curcumin or curcumin NP did not cause any alteration in the morphology of its epithelial and endothelial cells therefore can be safely applied to cornea via topical route.

Thus, we conclude curcumin-loaded MePEG-PCL NPs are potential candidates for prevention of corneal neovascularization.

Conflict of interest　The authors declare no conflict of interests related to this study.

References

1. Ambati BK, Nozaki M, Singh N, Takeda A, Jani PD, Suthar T, Albuquerque RJ, Richter E, Sakurai E, Newcomb MT et al (2006) Corneal avascularity is due to soluble VEGF receptor-1. Nature 443:993–997

2. Cursiefen C, Chen L, Saint-Geniez M, Hamrah P, Jin Y, Rashid S, Pytowski B, Persaud K, Wu Y, Streilein JW et al (2006) Proc Natl Acad Sci U S A 103:11405–11410

3. Amano S, Rohan R, Kuroki M, Tolentino M, Adamis AP (1998) Requirement for vascular endothelial growth factor in wound- and inflammation-related corneal neovascularization. Invest Ophthalmol Vis Sci 39:18–22

4. Cursiefen C, Chen L, Borges LP, Jackson D, Cao J, Radziejewski C, D'Amore PA, Dana MR, Wiegand SJ, Streilein JW (2004) VEGF-A stimulates lymphangiogenesis and hemangiogenesis in inflammatory neovascularization via macrophage recruitment. J Clin Invest 113:1040–1050

5. Gong Y, Koh DR (2010) Neutrophils promote inflammatory angiogenesis via release of preformed VEGF in an in vivo corneal model. Cell Tissue Res 339:437–448

6. Philipp W, Speicher L, Humpel C (2000) Expression of vascular endothelial growth factor and its receptors in inflamed and vascularized human corneas. Invest Ophthalmol Vis Sci 41:2514–2522

7. Gan L, Fagerholm P, Palmblad J (2004) Vascular endothelial growth factor (VEGF) and its receptor VEGFR-2 in the regulation of corneal neovascularization and wound healing. Acta Ophthalmol Scand 82:557–563

8. Benelli U, Ross JR, Nardi M, Klintworth GK (1997) Corneal neovascularization induced by xenografts or chemical cautery: inhibition by cyclosporin A. Invest Ophthalmol Vis Sci 38:274–282

9. Hayashi A, Popovich KS, Kim HC, de Juan E (1997) Role of protein tyrosine phosphorylation in rat corneal neovascularization. Graefes Arch Clin Exp Ophthalmol 235:460–467

10. Lee P, Wang CC, Adamis AP (1998) Ocular neovascularization: an epidemiologic review. Surv Ophthalmol 43:245–269

11. Gonzalez L, Loza RJ, Han KY, Sunoqrot S, Cunningham C, Purta P, Drake J, Jain S, Hong S, Chang JH (2013) Nanotechnology in corneal neovascularization therapy—a review. J Ocul Pharmacol Ther 29:124–134

12. Sarchahi AA, Maimandi A, Tafti AK, Amani M (2008) Effects of acetylcysteine and dexamethasone on experimental corneal wounds in rabbits. Ophthalmic Res 40:41–48

13. Guidera AC, Luchs JI, Udell IJ (2001) Keratitis, ulceration, and perforation associated with topical nonsteroidal anti-inflammatory drugs. Ophthalmology 108:936–944

14. Shakiba Y, Mansouri K, Rezaei N, Arshadi D (2009) Corneal neovascularization: molecular events and therapeutic options. Recent Patents Inflamm Allergy Drug Discov 3:221–231

15. Koenig Y, Bock F, Kruse FE, Stock K, Cursiefen C (2012) Angioregressive pretreatment of mature corneal blood vessels before keratoplasty: fine-needle vessel coagulation combined with anti-VEGFs. Cornea 31:887–892

16. Kim SW, Ha BJ, Kim EK, Tchah H, Kim TI (2008) The effect of topical bevacizumab on corneal neovascularization. Ophthalmology 115:33–38

17. Oh JY, Kim MK, Wee WR (2009) Subconjunctival and intracorneal bevacizumab injection for corneal neovascularization in lipid keratopathy. Cornea 28:1070–1073

18. Ambati BK, Anand A, Joussen AM, Kuziel WA, Adamis AP, Ambati J (2003) Sustained inhibition of corneal neovascularization by genetic ablation of CCR5. Invest Ophthalmol Vis Sci 44:590–593

19. Ambati BK, Joussen AM, Anand A, Adamis AP, Ambati J (2003) Inhibition of corneal neovascularization by genetic ablation of CCR2. Cornea 22:465–467

20. Lu P, Li L, Liu G, van Rooijen N, Mukaida N, Zhang X (2009) Opposite roles of CCR2 and CX3CR1 macrophages in alkali-induced corneal neovascularization. Cornea 28:562–569

21. Lan W, Petznick A, Heryati S, Rifada M, Tong L (2012) Nuclear factor-kB: central regulator in ocular surface inflammation and diseases. Ocul Surf 10:137–148

22. Zhao F, Gong Y, Hu Y, Lu M, Wang J, Dong J, Chen D, Chen L, Fu F, Qiu F (2015) Curcumin and its major metabolites inhibit the inflammatory response induced by lipopolysaccharide: translocation of nuclear factor-κB as potential target. Mol Med Rep 11: 3087–3093

23. Gaudana R, Jwala J, Boddu SH (2009) Recent perspectives in ocular drug delivery. Pharm Res 26:1197–1216

24. Chang JH, Gabison EE, Kato T (2001) Corneal neovascularization. Curr Opin Ophthalmol 12:242–249

25. Rawas-Qalaji M, Williams CA (2012) Advances in ocular drug delivery. Curr Eye Res 37:345–356

26. Guha R, Chowdhury S, Palui H, Mishra A, Basak S, Mandal TK, Hazra S, Konar A (2013) Doxorubicin-loaded MePEG-PCL nanoparticles for prevention of posterior capsular opacification. Nanomedicine (Lond) 8:1415–1428

27. Qazi Y, Stagg B, Singh N, Singh S, Zhang X, Luo L, Simonis J, Kompella UB, Ambati BK (2012) Nanoparticle-mediated delivery of shRNA. VEGF-A plasmids regresses corneal neovascularization. Invest Ophthalmol Vis Sci 53:2837–2844

28. Al-Abd AM, Kim NH, Song SC, Lee SJ, Kuh HJ (2009) A simple HPLC method for doxorubicin in plasma and tissues of nude mice. Arch Pharm Res 32:605–611

29. Bian F, Zhang MC, Zhu Y (2008) Inhibitory effect of curcumin on corneal neovascularization in vitro and in vivo. Ophthalmologica 222:178–186

30. Klein R, Lobes LA Jr (1976) Ocular alkali burns in a large urban area. Ann Ophthalmol 8:1185–1189

31. Morgan SJ (1987) Chemical burns of the eye: causes and management. Br J Ophthalmol 71:854

32. Huang FC, Chan WK, Moriarty KJ (1998) Novel cytokine release inhibitors. Part I: triterpenes. Bioorg Med Chem Lett 8:1883–1886

33. Kim JS, Choi JS, Chung SK (2010) The effect of curcumin on corneal neovascularization in rabbit eyes. Curr Eye Res 35:274–280

34. Sivak JM, Ostriker AC, Woolfenden A, Demirs J, Cepeda R, Long D, Anderson K, Jaffee B (2011) Pharmacologic uncoupling of angiogenesis and inflammation during initiation of pathological corneal neovascularization. J Biol Chem 286:44965–44975

35. Ma DH, Chen JK, Kim WS, Hao YX, Wu HC, Tsai RJ, Hwang DG, Zhang F (2001) Expression of matrix metalloproteinases 2 and 9 and tissue inhibitors of metalloproteinase 1 and 2 in inflammation-induced corneal neovascularisation. Ophthalmic Res 33:353–362

36. Arbiser JL, Klauber N, Rohan R, van Leeuwen R, Huang MT, Fisher C, Flynn E, Byers HR (1998) Curcumin is an in vivo inhibitor of angiogenesis. Mol Med 4:376–383

37. Gao C, Ding Z, Liang B, Chen N, Cheng D (2003) Study on the effects of curcumin on angiogenesis. Zhong Yao Cai 26:499–502

38. Gupta SK, Kumar B, Nag TC (2011) Curcumin prevents experimental diabetic retinopathy in rats through its hypoglycemic, antioxidant, and anti-inflammatory mechanisms. J Ocul Pharmacol Ther 27:123–130

39. Anand P, Kunnumakkara AB, New-man RA, Aggarwal BB (2007) Bioavailability of curcumin: problems and promises. Mol Pharm 4: 807–818